Atomic Contributions to the Optical Rotation Angle as a Quantitative Probe of Molecular Chirality

Rama K. Kondru, Peter Wipf, David N. Beratan

Chiral molecules are characterized by a specific rotation angle, the angle through which plane-polarized light is rotated on passing through an enantiomerically enriched solution. Recent developments in methodology allow computation of both the sign and the magnitude of these rotation angles. However, a general strategy for assigning the individual contributions that atoms and functional groups make to the optical rotation angle and, more generally, to the molecular chirality has remained elusive. Here, a method to determine the atomic contributions to the optical rotation angle is reported. This approach links chemical structure with optical rotation angle and provides a quantitative measure of molecular asymmetry propagation from a center, axis, or plane of chirality.

The rotation of plane-polarized light by a solution of chiral molecules arises from the difference in the index of refraction for left and right circularly polarized light (*1*). Optical rotation is measured as a function of frequency in optical rotatory dispersion spectra. It is probed routinely at a single frequency in organic laboratory polarimetry measurements of the rotation angle. This angle depends on chemical bonding and molecular conformation in a complex and as yet poorly understood way.

Linking the rotation angle to molecular structure is a challenge of fundamental as well as practical importance. For example, the chemical bonding pattern is often known for natural and synthetic products of potential use in medicine, but it can be challenging to determine the absolute handedness of every chiral center. When N stereocenters are present, there are 2^N possible stereoisomers for a structure. Yet, an unambiguous assignment of absolute stereochemistry is essential for a reproducible laboratory synthesis or a meaningful structure-activity study. The assignment of absolute stereochemistry is particularly problematic in large flexible molecules of novel structure containing multiple chiral centers.

Since van't Hoff (*2*) and Le Bel (*3*) related the phenomenon of optical rotation to the presence of asymmetric carbon atoms, empirical (*4*, *5*), semiempirical (*6*–*9*), classical (*10*), and quantum mechanical (*11*–*16*) models have been developed to describe the theoretical origin of the rotation angle. Valuable conceptual advances were made, as well, in defining chirality functions (*17*).

Department of Chemistry, University of Pittsburgh, Pittsburgh, PA 15260, USA.

Very recently, quantitatively reliable quantum computations of molar rotation angles have become available (*18*–*21*). The basic theoretical framework governing chiroptical phenomena in molecules, however, has been known since the early days of quantum mechanics. Rosenfeld and Condon described the quantum mechanical origins of the optical rotation angle (*23*). Early models of Kirkwood and others (*8*, *11*, *24*) were based largely on interacting polarizable atoms or chemical groups. These models are instructive and may succeed in predicting some rotation angles in limited families of structures, but no general strategy exists for assigning the contributions of individual atoms (or chemical groups) to the optical rotation angle. Also, no reliable empirical rules exist yet for predicting either the sign or order of magnitude of the optical rotation angle for molecules of known structure. Here, we present a quantitative method to dissect the optical rotation angle into its individual atomic contributions. This atomic mapping protocol provides a foundation for establishing fundamental relations between chemical structure and optical rotation angles in molecules and links modern quantitatively reliable computation to numerous empirical models developed over the past 100 years. Moreover, this analysis provides a precise measure for the magnitude and the decay of asymmetry in the vicinity of an asymmetric unit in a molecule. The present analysis complements earlier work from our group (*20*) and from Polavarapu's group (*19*, *21*) that assigned absolute stereochemistry on the basis of a comparison of computed and observed molar rotation angles and demonstrated the numerical reliability of the computations (*25*, *26*). We use full molecule computations to resolve the specific rotation of a molecule into its individual atomic contributions. Our strategy is conceptually distinct from previous atom-based analyses that extrapolated parameters taken from single atoms or molecular fragments (*5*, *7*, *11*).

The optical rotatory parameter β is related to the angular frequency of the incident radiation (ω) and the elements of the electric dipole–magnetic dipole polarizability tensor G' (*23*) as

$$\beta = -\omega^{-1}(G'_{xx} + G'_{yy} + G'_{zz})/3 \quad (1)$$

The specific rotation angle (*21*) (measured at the sodium D line), usually reported in units of degree [decimeters (g/ml)]$^{-1}$, is

$$[\alpha]_D = 1.343 \times 10^{-4}\, \beta \bar{\nu}^2\, (n^2 + 2)/3MW \quad (2)$$

where β is in units of (bohr)^4, MW is the molar mass in grams per mole, n is the refractive index of the medium, and $\bar{\nu}$ is the frequency of the sodium D line in cm^{-1}. From $[\alpha]_D$, the molar rotation is defined as $[M]_D = [\alpha]_D MW/100$. We calculate G' (*14*) for the full molecule using

$$G'_{\alpha\alpha} = -2\omega \mathrm{Im} \sum_{e \neq g} \frac{\langle \Psi_g^{(0)} | \mu_\alpha | \Psi_e^{(0)} \rangle \langle \Psi_e^{(0)} | m_\alpha | \Psi_g^{(0)} \rangle}{\omega_{eg}^2 - \omega^2} \quad (3)$$

where $\Psi_g^{(0)}$ and $\Psi_e^{(0)}$ denote the ground and excited state wave functions, respectively, and $\omega_{eg} = \omega_e - \omega_g$ is the associated excitation frequency. μ_α and m_α are the electric and magnetic dipole operators, respectively, oriented along the α axis. Equation 3 can be simplified in the limit where the incident radiation frequency is far from promoting any resonant electronic absorption (*27*). In that case, $\omega^2 \ll \omega_{eg}^2$, and if we write $\omega_{eg} = (E_e^{(0)} - E_g^{(0)})$ (where $E_e^{(0)}$ are the excited state energies and $E_g^{(0)}$ are the ground state energies of the unperturbed wave functions),

$$\omega^{-1} G'_{\alpha\alpha} = -2\mathrm{Im} \sum_{e \neq g} \left\{ \frac{\langle \Psi_g^{(0)} | \mu_\alpha | \Psi_e^{(0)} \rangle}{(E_e^{(0)} - E_g^{(0)})} \right\} \left\{ \frac{\langle \Psi_e^{(0)} | m_\alpha | \Psi_g^{(0)} \rangle}{(E_e^{(0)} - E_g^{(0)})} \right\} \quad (4)$$

For a single determinant wave function, first-order changes to the ground state are described in terms of perturbations to the molecule's occupied molecular orbitals (ψ_n) by the electric (E) and magnetic (B) fields. These perturbations are closely related to the two bracketed terms in Eq. 4,

$$\frac{\partial \psi_n}{\partial E_\alpha} = \sum_{j \neq n} \left\{ \frac{\langle \psi_n^{(0)} | \mu_\alpha | \psi_j^{(0)} \rangle}{(E_j^{(0)} - E_n^{(0)})} \right\} \psi_j^{(0)} = \sum_{j \neq n} P_{nj}\, \psi_j^{(0)} \quad (5a)$$

$$\frac{\partial \psi_n}{\partial B_\alpha} = \sum_{j \neq n} \left\{ \frac{\langle \psi_n^{(0)} | m_\alpha | \psi_j^{(0)} \rangle}{(E_j^{(0)} - E_n^{(0)})} \right\} \psi_j^{(0)} = \sum_{j \neq n} Q_{nj} \psi_j^{(0)} \quad (5b)$$

where n and j represent the occupied and unoccupied molecular orbitals, respectively. The P and Q elements are computed routinely with coupled-perturbed Hartree-Fock methods (*26*). Finally, expanding the molecular orbitals $\psi_j^{(0)}$ as a linear combination of atomic orbitals (ϕ_l) according to $\psi_j^{(0)} = \Sigma_l C_{jl} \phi_l$ and substituting $\psi_j^{(0)}$ into Eq. 5 yield

$$\frac{\partial \psi_n}{\partial E_\alpha} = \sum_{j \neq n} P_{nj} \sum_l C_{nl} \phi_l = \sum_l P'_{nl} \phi_l \quad (6a)$$

$$\frac{\partial \psi_n}{\partial B_\alpha} = \sum_{j \neq n} Q_{nj} \sum_k C_{nk} \phi_k = \sum_k Q'_{nk} \phi_k \quad (6b)$$

These two wave function derivatives describe the way that the molecular orbitals change upon application of the E and B fields. Inserting these derivatives into Eq. 4 gives an expression for the G' elements in terms of atomic orbital overlaps and the computed molecular orbital coefficients:

$$\omega^{-1} G'_{\alpha\alpha} = -2\mathrm{Im}\left\{ \sum_n \left\langle \frac{\partial \psi_n}{\partial E_\alpha} \middle| \frac{\partial \psi_n}{\partial B_\alpha} \right\rangle \right\} = -2 \sum_n \sum_{l,k} P'_{nl} Q'_{nk} \langle \phi_l | \phi_k \rangle \quad (7)$$

This expression can be analyzed in a manner analogous to Mulliken population analysis (*28*). The diagonal terms ($l = k$) represent pure atomic contributions to the G' tensor. Off-diagonal terms ($l \neq k$) describe the bonding and through-space contributions, which we divide equally between each pair of contributing atoms (*28*).

The coupled-perturbed Hartree-Fock strategy computes the ground state wave function perturbations (all at once, without the use of fragmentation schemes) and is quantitatively reliable for molecules of modest size (*19*, *21*). From these perturbations, we then compute the atomic contributions to the rotation angle using Eq. 7.

As a first demonstration of this strategy, achiral oxirane and chiral substituted oxiranes were chosen for their simplicity and rigidity. The atomic contributions to the molar rotation angles in fluorooxirane, chlorooxirane, bromooxirane and methyloxirane were computed with 6-31G** basis set (*29*) optimized geometries; the same basis was used in the rotation-angle calculations. Our analysis characterizes each atomic (or group) contribution to the optical rotation angle. A large contribution from the center of asymmetry in all molecules and a more modest contribution from the oxygen atom are demonstrated in Fig. 1. Even though fluorine is directly bound to the asymmetric carbon, it does not contribute substantially to the rotation angle itself (Fig. 1B). In contrast, the atomic contributions of the more polarizable chlorine and bromine atoms are large (Fig. 1, C and D). For substituted oxiranes for which an experimental value of $[M]_D$ is known, the overall computed value is in good agreement with the experimental value (*19*, *30*), indicating that our atomic-level analysis is quantitatively reliable.

Chiral 2,7,8-trioxabicyclo[3.2.1] octanes (Scheme 1, **1** to **3**) have attracted theoretical interest because of their conformational rigid-

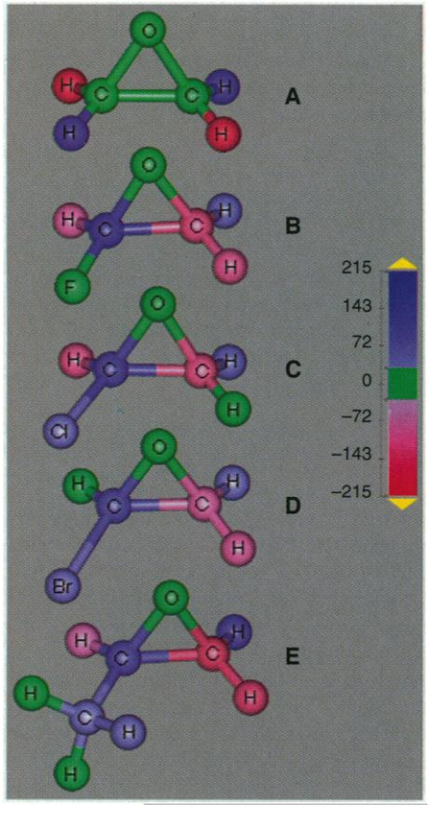

Fig. 1. Atomic contributions to the molar rotation in oxirane and in four substituted oxiranes: (**A**) oxirane, (**B**) fluorooxirane, (**C**) chlorooxirane, (**D**) bromooxirane, and (**E**) methyloxirane. The atoms are colored according to their contribution to the molar rotation angle. Atoms shown in green carry small or no contribution, atoms in red have a negative contribution, and those in blue have a positive contribution to the molar rotation angle. Note the canceling hydrogen contributions in oxirane (A). In the other molecules, the chiral carbon carries a large contribution, and the oxygen in the ring carries a smaller contribution. The halogen contribution increases with the size of the halogen. In fluorooxirane (B), the fluorine contribution is small, in contrast to the larger bromine contribution in bromooxirane (D). The sum of all atomic contributions shown for each molecule represents the molar rotation (as calculated in the coupled Hartree-Fock analysis that leads to these plots). In this series of molecules, a 6-31G** basis set was used to calculate the optical rotation angles and their atomic contributions.

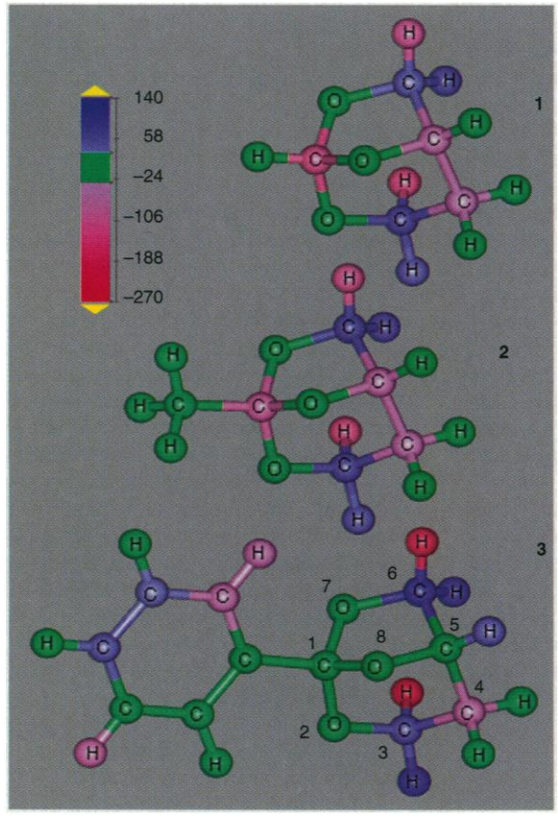

Fig. 2. For the substituted bicyclic orthoesters **1** to **3**, the same color scheme as in Fig. 1 is used (a 4-31G* basis set was used for computation of rotation angles and atomic contributions). The hydrogen atom connected to the bridgehead C1 in **1** carries a very small contribution. Similarly, the methyl group connected to C1 in **2** has a small contribution. In these compounds, oxygen atoms are green, indicating little contribution to the molar rotation angle. The twisted butane fragment, C3-C4-C5-C6, and the phenyl ring make an important contribution to the sign and magnitude of the molar rotation angle in these compounds.

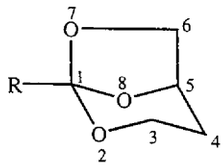

1, R=H

2, R=Me

3, R=Ph

Scheme 1.

ity and the availability of x-ray crystal structures (*31*). On the basis of the calculated and experimental molar rotation angles of **1** to **3**, Applequist *et al.* (*31*) showed that the rotation angle is apparently insensitive to substitution at the bridgehead carbon. Applequist's model predicts a modest dependence on the ring orientation in **3**. We compared the calculated molar rotation angles of **1** to **3** according to Applequist's atom-dipole interaction model (*7*, *31*) and those determined by our ab initio coupled Hartree-Fock calculations in the 6-31G, 6-31G*, and 4-31G* basis sets (*26*) (Table 1). The atom-dipole calculations predict the correct sign of the rotation angle, but the computed magnitude is about four times the experimental values in all compounds. Our Hartree-Fock 4-31G* quantum mechanical calculations, in contrast, provide excellent agreement with all experimental data.

Applequist suggested that the lack of dependence on the type and orientation of the bridgehead substituent arose from its distance from the gauche C3-C4-C5-C6 unit, whose contribution to the rotation angle was suspected to exceed that of the bridgehead carbon itself. Our atomic analysis is well suited to examine this hypothesis and to identify the atomic origin of optical rotations (Fig. 2).

Note that the atoms in **1** to **3** contribute to different degrees. In compounds **1** and **2**, the twisted butane moiety, C3-C4-C5-C6, provides the dominant contribution, consistent with Applequist's hypothesis, although the quantitative agreement is substantially better in the present study. In contrast, in compound **3**, both the phenyl group and the twisted butane moiety make substantial atomic contributions, counter to the predictions of the empirical model. Rather than the asymmetric carbon C(1) exclusively, the conformationally locked chiral butane substructure (and the phenyl ring) dominate the rotation of plane-polarized light in these molecules.

As a final example, we considered CH_2 and CH_3 group contributions to the optical rotation in a molecule that contains a single chiral center connected to an alkyl chain. 2-Fluorohexane was analyzed in two configurations (Fig. 3), one extended and one somewhat folded. Van't Hoff's principle of optical superposition (*2*) suggests that asymmetric centers separated by several single bonds make simple additive contributions to the molar rotation angle (*1*, *2*). The rapid decay of atomic contributions to the optical rotation in the extended geometry accounts qualitatively for van't Hoff's observation. The folded geometry introduces conformational asymmetry in the carbon chain, resulting in atoms remote from the chiral carbon also making substantial contributions to the molar rotation angle (Fig. 4). The atomic maps allow detailed analysis of how molecular conformation affects optical rotation.

We have introduced a method for calculating atomic and group contributions to the optical rotational angle of a chiral molecule. The resulting atom-based structure-function relations can reveal the structural and geometric sensitivity of the rotation angle, as well as measure subtle substituent and chemical bonding effects. This correlation between molecular structure and macroscopic phenomena may help to establish polarization rotation design principles for use in materials research and may facilitate data analysis in chiroptical spectroscopy (*32*). Moreover, atomic analyses of optical rotation may help to establish new quantitative definitions of molecular asymmetry and the nature of its propagation through bonds and through space.

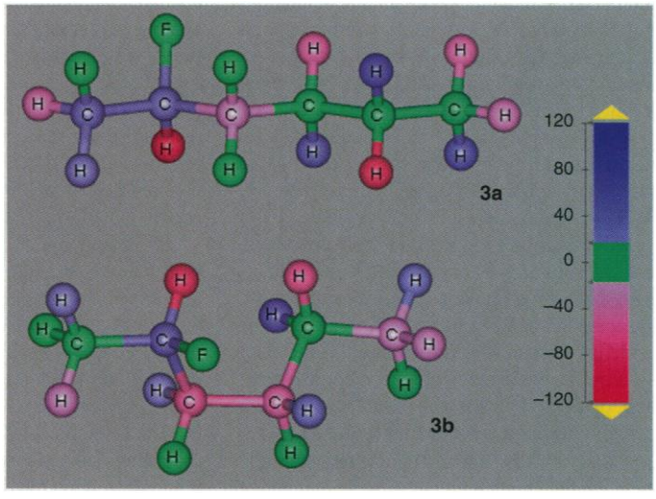

Fig. 3. Atomic contributions to the molar rotation angle in 2-fluorohexane in the configurations **3a** (~180° dihedral angle) and **3b** (~60° dihedral angle). In the extended geometry, the rapid decay of CH_2 group contributions to the rotation angle is marked (the first methylene unit contributes half as much as the CHF unit, and the second methylene contributes only 10% of the CHF unit; see Fig. 4). In the gauche configuration **3b**, because of conformational asymmetry in the carbon chain, atoms that are farther away from the chiral carbon also contribute substantially to the molar rotation angle of this conformer.

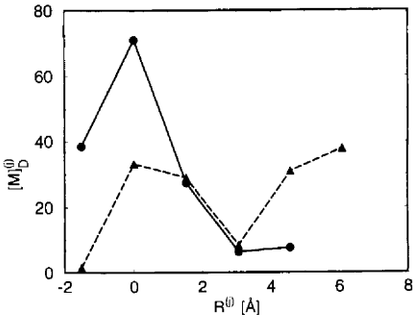

Fig. 4. Absolute value of the group (CH_2 or CH_3) contributions to the molar rotation angle $[M]_D^{(j)}$ (in degrees) in 2-fluorohexane as a function of carbon atom distance from the chiral center ($R^{(j)}$), in **3a** and **3b**. The solid line shows the rapid decay of group contributions as a function of distance in the extended geometry (**3a**), and the dashed line shows the group contributions for the gauche conformation (**3b**) (~60° dihedral angle). The rapid decay with distance in **3a** is consistent with the empirical observation that chiral centers separated by several single bonds have an additive effect on the observed rotation angle. The lack of decay in **3b** arises from the chain's conformational asymmetry, which is spread over the entire folded molecule.

Table 1. Calculated molar rotation angles (in degrees) of **1** to **3** according to Applequist's atom-dipole interaction model (*7*, *31*) and our ab initio coupled Hartree-Fock calculations in the 6-31G, 6-31G*, and 4-31G* basis sets (*26*).

Compound	Applequist	6-31G	6-31G*	4-31G*	Experimental values (*31*)
1	−404	−129	−139	−153	−145.2
2	−508	−108	−116	−132	−120.5
3	−427	−73	−97	−118	−121.5

References and Notes

1. E. L. Eliel, S. H. Wilen, L. N. Mander, *Stereochemistry of Organic Compounds* (Wiley, New York, 1994).
2. J. H. van't Hoff, *Die Lagerung der Atome im Raume* (Vieweg, Braunschweig, Germany, 1894); *Arch. Neerl. Sci. Exactes Nat.* **9**, 455 (1874).
3. J. A. Le Bel, *Bull Soc. Chim. Fr.* **22**, 337 (1874).
4. P. Walden, *Z. Phys. Chem.* **15**, 196 (1894); K. Freudenberg, J. Todd, R. Seidler, *Ann. Chem.* **501**, 199 (1933).
5. J. H. Brewster, *Tetrahedron* **13**, 106 (1961).
6. A. Moscowitz, *Adv. Chem. Phys.* **4**, 67 (1962).
7. J. Applequist, *J. Chem. Phys.* **58**, 4251 (1973); *Acc. Chem. Res.* **10**, 79 (1977).
8. I. J. Tinoco and R. W. Woody, *J. Chem. Phys.* **40**, 160 (1963).
9. Y. H. Pao and D. P. Santry, *J. Am. Chem. Soc.* **88**, 4157 (1966); R. R. Gould and R. Hoffmann, *ibid.* **92**, 1813 (1970); B. K. Satyanarayana and E. S. Stevens, *J. Org. Chem.* **52**, 3170 (1987).
10. W. Kuhn, in *Stereochemie*, K. Freudenberg, Ed. (Deuticke, Leipzig, Germany, 1933), vol. 8, p. 394; M. Born, *Proc. R. Soc. London A* **150**, 84 (1935).
11. J. G. Kirkwood, *J. Chem. Phys.* **5**, 479 (1937).
12. R. K. Kondru, S. Lim, P. Wipf, D. N. Beratan, *Chirality* **9**, 469 (1997).
13. A. Rauk and J. M. Barriel, *Chem. Phys.* **25**, 409 (1977).
14. K. L. Bak *et al.*, *Theor. Chim. Acta* **90**, 441 (1995); A. E. Hansen and T. D. Bouman, *J. Am. Chem. Soc.* **107**, 4828 (1985).
15. G. Snatzke, in *Chirality, from Weak Bosons to the Alpha Helix*, R. Janoschek, Ed. (Springer-Verlag, Berlin, 1991), pp. 59–85.
16. K. Nakanishi, N. Berova, R. W. Woody, *Circular Dichroism: Principles and Applications* (VCH, New York, 1994).
17. E. Ruch, W. Runge, G. Kresze, *Angew. Chem. Int. Ed. Engl.* **12**, 30 (1973); E. Ruch, *ibid.* **16**, 65 (1977); *Acc. Chem. Res.* **5**, 49 (1972).
18. J. Costante, L. Hecht, P. L. Polavarapu, A. Collet, L. D. Barron, *Angew. Chem. Int. Ed. Engl.* **36**, 885 (1997).
19. P. L. Polavarapu, *Tetrahedron Asymmetry* **8**, 3397 (1997); *Mol. Phys.* **91**, 551 (1997).
20. R. K. Kondru, P. Wipf, D. N. Beratan, *J. Am. Chem. Soc.* **120**, 2204 (1998).
21. P. L. Polavarapu and D. K. Chakraborty, *ibid.*, p. 6160.
22. A. Lakhtakia, *Selected Papers on Natural Optical Activity* (SPIE Press, Bellingham, WA, 1990), vol. MS15.
23. L. Rosenfeld, *Z. Phys.* **52**, 161 (1928).
24. W. Moffitt, *J. Chem. Phys.* **25**, 467 (1956).
25. T. Helgaker *et al.*, Dalton, an ab initio electronic structure program, version 1.0 (1997).
26. R. D. Amos and J. E. Rice, *The Cambridge Analytic Derivative Package*, version 4.0 (1987), and the basis sets listed in the CADPAC library.
27. R. D. Amos, *Chem. Phys. Lett.* **87**, 23 (1982); *ibid.* **124**, 376 (1986).
28. R. S. Mulliken, *J. Chem. Phys.* **23**, 1833 (1955); *ibid.* **36**, 3428 (1962); J. A. Pople and D. L. Beveridge, *Approximate Molecular Orbital Theory* (McGraw-Hill, New York, 1970). As in assigning atomic charges, there is some ambiguity in defining atomic contributions to G'. Here, we divide off-diagonal terms equally between participant atoms.
29. M. J. Firsch *et al.*, Gaussian 94, rev. C.2 (1995), and the basis sets used in the Gaussian program library.
30. The computed specific rotation angle for (*R*)-2-methyloxirane with the CADPAC program is 24 compared with an experimental value of 14.0, and the computed specific rotation angle for *trans*-(2*R*,3*R*)-dimethyloxirane is 45 compared with an experimental value of 58.8. The computed molar rotation angle for (*S*)-fluorooxirane is –36.
31. A. E. Wroblewski *et al.*, *J. Am. Chem. Soc.* **110**, 4144 (1988).
32. R. McKendry, M. E. Theoclitou, T. Rayment, C. Chris, *Nature* **391**, 566 (1998); T. A. Jung, R. R. Schlittler, J. K. Gimzewski, *ibid.* **386**, 696 (1997).

33. We thank the PRF (33532AC), NSF (CHE-9727657), and NIH (GM 55433-04) for support of this research and D. W. Pratt for helpful discussions.

14 September 1998; accepted 16 November 1998

Behavioral State Modulation of Auditory Activity in a Vocal Motor System

Amish S. Dave, Albert C. Yu, Daniel Margoliash*

Neurons of the song motor control nucleus robustus archistriatalis (RA) exhibited far weaker auditory responses in awake than in anesthetized zebra finches. Remarkably, sleep induced complex patterns of bursts in ongoing activity and uncovered vigorous auditory responses of RA neurons. Local injections of norepinephrine suggested that the changes in response strength occur through neuromodulatory control of the sensorimotor nucleus HVc, which projects to RA. Thus, motor access to auditory feedback, which zebra finches require for song learning and maintenance, may be regulated through neuromodulation. During sleep, the descending motor system may gain access to sensorimotor song memories represented as bursting patterns of activity.

Changes in behavioral state are accompanied by changes in the functional properties of forebrain neurons. As animals transition to sleep, neurons may exhibit reduced responsiveness to external stimuli, reduced ongoing ("spontaneous") firing rates, and increased bursting and synchronization. The cellular mechanisms for such changes are mediated by the actions of neuromodulators, including norepinephrine (*1*). Behavioral and comparative studies have suggested that sleep may play a role in the stabilization of certain types of memory, including the learning of fine motor tasks, but, in general, the behavioral implications of sensory gating are not as well established (*2*). Here we report that neuromodulatory regulation within the bird vocal motor ("song") system controls the expression of activity patterns associated with learned auditory information. In contrast to the pattern typical for other systems, sensory responsiveness increases during sleep.

Song learning requires auditory feedback, and the role of auditory feedback is modulated during development (*3*). In the forebrain, the nucleus HVc and its afferents are the principal targets of auditory input to the song system (*4*). Neurons in HVc project to one of two pathways, either the descending motor pathway through a projection to the forebrain nucleus robustus archistriatalis (RA) or the anterior forebrain pathway (AFP) that eventually projects back to RA (Fig. 1A). Whereas HVc and RA are necessary for singing, the AFP is necessary for the development of normal song, but lesions of AFP nuclei in the adult have little effect on singing in zebra finches (*5*).

We recorded single neurons in the HVc and RA of awake, freely moving animals (*6*). Numerous previous studies, mostly conducted in urethane-anesthetized animals, have shown that HVc (*7, 8*) and RA and AFP (*8*) neurons have auditory responses that are specific for acoustic features of the individual bird's own song (BOS) and are selective for BOS relative to conspecific songs. We also observed such selectivity in the auditory responses of single HVc neurons in awake birds but, surprisingly, failed to observe any auditory response whatsoever in RA neurons recorded under the same conditions (*9*). The RA neurons exhibited fast regular oscillatory spiking patterns that lacked the occasional bursts observed in recordings from anesthetized birds. The complete absence of an auditory response in RA may have been the result of a neuromodulatory response related to stress induced during a brief period when the animals were manually restrained to achieve single-unit isolation (*6*) (see below).

Exploring under what behaviorally relevant conditions RA neurons exhibited the auditory responsiveness observed in anesthetized animals, we discovered that when birds fell asleep, RA neurons acquired complex bursting in their ongoing activity and, remarkably, gained auditory responsiveness to BOS. At night, birds prepared for chronic recordings of RA neurons were presented with continuous playback of BOS (*6*). When the cage lights were turned off, motion in the cage (as judged by lack of audible movements) eventually ceased and the birds fell asleep. Without fail, sleep was accompanied by slower, less regular firing (14 single units, five birds; Fig. 1B) and a dramatic increase in the auditory response to BOS (10 of 14 single units and six multiple units in four birds were tested); the effect was sufficiently reliable to be easily seen in multiple unit traces (Fig. 1D). The RA "sleep" state of ongoing activity and BOS responsiveness was observed whenever we sampled RA during the night. The only

Department of Organismal Biology and Anatomy, Committee on Neurobiology, University of Chicago, 1027 E. 57th Street, Chicago, IL 60637, USA.

* To whom correspondence should be addressed. E-mail: dan@bigbird.uchicago.edu